

Molecular Composition of Oxygenated Organic Molecules and Their Contributions to Organic Aerosol in Beijing

Yonghong Wang,* Petri Clusius, Chao Yan, Kaspar Dällenbach, Rujing Yin, Mingyi Wang, Xu-Cheng He, Biwu Chu, Yiqun Lu, Lubna Dada, Juha Kangasluoma, Pekka Rantala, Chenjuan Deng, Zhuohui Lin, Weigang Wang, Lei Yao, Xiaolong Fan, Wei Du, Jing Cai, Liine Heikkinen, Yee Jun Tham, Qiaozhi Zha, Zhenhao Ling, Heikki Junninen, Tuukka Petäjä, Maofa Ge, Yuesi Wang, Hong He, Douglas R. Worsnop, Veli-Matti Kerminen, Federico Bianchi, Lin Wang, Jingkun Jiang,* Yongchun Liu,* Michael Boy, Mikael Ehn, Neil M. Donahue, and Markku Kulmala*



Cite This: *Environ. Sci. Technol.* 2022, 56, 770–778



Read Online

ACCESS |

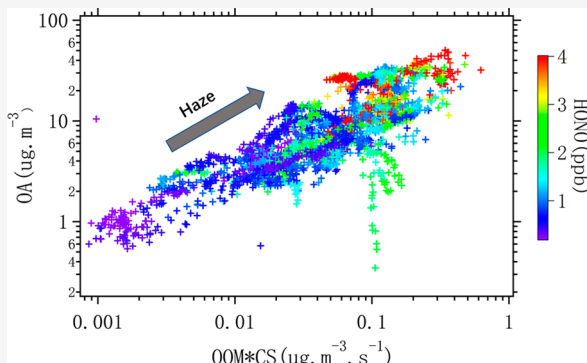
Metrics & More

Article Recommendations

Supporting Information

ABSTRACT: The understanding at a molecular level of ambient secondary organic aerosol (SOA) formation is hampered by poorly constrained formation mechanisms and insufficient analytical methods. Especially in developing countries, SOA related haze is a great concern due to its significant effects on climate and human health. We present simultaneous measurements of gas-phase volatile organic compounds (VOCs), oxygenated organic molecules (OOMs), and particle-phase SOA in Beijing. We show that condensation of the measured OOMs explains 26–39% of the organic aerosol mass growth, with the contribution of OOMs to SOA enhanced during severe haze episodes. Our novel results provide a quantitative molecular connection from anthropogenic emissions to condensable organic oxidation product vapors, their concentration in particle-phase SOA, and ultimately to haze formation.

KEYWORDS: air pollution, organic aerosol, haze, oxygenated organic molecules, volatility



INTRODUCTION

Air pollution in China has caused great concern due to its effect on human health and climate,^{1–4} although recent studies have revealed a remarkable reduction of particulate matter (PM) over eastern China since 2013.^{5,6} Secondary organic aerosol (SOA) is an important component of fine particulate matter and thus haze.⁷ On a global scale, gas-to-particle partitioning of low volatility organic compounds (LVOCs) is considered to be the main formation pathway of SOA, while aqueous-phase formation of LVOCs is a significant supplement to the global SOA burden.^{8–12} Especially in megacities of China, intense production of SOA is considered to be responsible for severe haze formation.^{13–15} Abundant organic vapors from anthropogenic emissions are oxidized by hydroxyl radicals (OH), nitrate radicals (NO₃), ozone (O₃), and chlorine atoms (Cl) and subsequently influenced by nitrogen oxides (NO_x), sulfur dioxide (SO₂), and ammonia (NH₃). The chemical system is extremely complicated, especially because of cross reactions between different peroxy radicals. It is difficult to elucidate urban organic aerosol formation at a molecular level, even in a well-controlled smog chamber.^{16–18}

Volatility of atmospheric organic vapors determines the preference of vapors for the gas or particle phase.^{19,20} Organic volatility is closely related to functional groups and oxidation state. Recently, formation of highly oxygenated organic molecules via autoxidation has been proposed as an important route for condensable vapor formation.²¹ The process is characterized by multiple intramolecular H atom shifts in peroxy radicals, each followed by rapid oxygen addition to form multifunctional peroxy radicals with a high oxidation extent.^{21–24} However, autoxidation may be limited in urban areas due to the high concentration of nitric oxide (NO).²⁵ Although the majority of peroxy radicals reacts with NO by forming alkoxy radicals and NO₂, the rapid reaction of NO with peroxy radicals will terminate the autoxidation process by forming closed-shell products. These products are less

Received: August 5, 2021

Revised: November 12, 2021

Accepted: November 12, 2021

Published: November 22, 2021



oxygenated and therefore semivolatile organic compounds (SVOCs), though LVOCs and also extremely low volatile organic compounds (ELVOCs) are still formed; consequently, this lowers the yield of LVOCs, which play a vital role in the growth of newly formed particles.^{17,21} However, multiple generations of oxidation may also be important under highly oxidizing conditions.^{26,27}

Online detection of highly oxygenated organic molecules at the subppt level only recently became possible with the development of the NO₃-Cl-APi-ToF, which is a novel instrument for measurement of gas-phase sulfuric acid and highly oxygenated organic molecules based on the selective and sensitive clustering of nitrate anions with hydroxyl and hydroperoxyl groups.^{21,28} However, as yet there have been few deployments of the NO₃-Cl-APi-ToF in the urban atmosphere to measure oxygenated organic compounds and their role in aerosol formation and growth.^{29–31} Organic aerosol associated with haze formation in Chinese megacities has been studied extensively with advanced online mass-spectrometer technology utilizing electron ionization.³² However, this approach only provides aerosol fragments and elementary information on bulk organic aerosol composition; knowledge about organic aerosol composition at the molecular level is still limited.

MATERIALS AND METHODS

Sampling Site. The measurements were conducted between March 3 and 30, 2018 on the rooftop of a university building on the west campus of the Beijing University of Chemical Technology (39.95° N, 116.31° E). This station is located about 150 m away from the nearest road (Zizhuyuan Road) and 500 m away from the West Third Ring Road. The station is surrounded by commercial properties and residential dwellings and is thus representative of a typical urban environment.

Measurement of OOMs and Calibration. Oxidized organic molecules are measured by a chemical ionization long time-of-flight mass spectrometer (LToF-CIMS, Aerodyne Research, Inc.) equipped with a nitrate chemical ionization source.²⁸ Ambient air is drawn into the ionization source through a stainless-steel tube with a length of 1.6 m and a diameter of 3/4 in. A mixture of a 3 mL min⁻¹ ultrahigh purity nitrogen flow containing nitric acid and a 20 L min⁻¹ pure air flow supplied by a zero-air generator (Aadco 737, USA), together as a sheath flow, is guided through a PhotoIonizer (Model L9491, Hamamatsu, Japan) to produce nitrate reagent ions. This sheath flow is then introduced into a coaxial laminar flow reactor concentric to the sample flow. Nitrate ions are pushed to the sample flow layer by an electric field and subsequently charge analyte molecules. Throughout the campaign, the sample flow rate is kept at 8.8 L min⁻¹, out of which about 0.8 L min⁻¹ is drawn through the pinhole into the TOF module, and the rest is extracted by vacuum. We use 1.1 × 10¹⁰ molecules cm⁻³ as the calibration coefficient after taking into account the diffusion loss of OOMs in the 1.6 m sampling line.

Estimation of organic vapor concentration includes two steps. First, a mass-dependent transmission correction is performed. Such mass-dependency is instrument-specific and is influenced by many instrumental parameters. This transmission bias is determined by depleting the primary ion with a series of perfluorinated acids and comparing the primary ion signal depletion with the product signal increase (which would match for equivalent transmission efficiency). The detailed

method was described in a previous study.³³ Second, we apply the calibration coefficient determined for sulfuric acid to estimate the organic vapor concentration.

For the OOMs measured here, we assume that NO₃⁻ clustering has the same rate coefficient as the sulfuric acid ion transfer reaction (i.e., both are collision limited), which is supported for ELVOC and ULVOC multifunctional organics in the literature.²¹ Because the OOMs form clusters with NO₃⁻, we have removed the NO₃⁻ from all of the reported ion masses and chemical formulas reported here.

Measurement of Organic Aerosol, Calibration, and Sources Apportionment with PMF. Online Time-of-Flight Aerosol Chemical Speciation Monitor (ToF-ACSM, equipped with a standard vaporizer) observations were conducted at the BUCT station from February 21 to April 7, 2018, equipped with a PM_{2.5} lens.³⁴ The nonrefractory fraction of fine-particle mass concentrations (NR-PM_{2.5}, including organics, sulfate, nitrate, ammonium, and chloride) was obtained by the ToF-ACSM standard data analysis software (Tofware) within Igor Pro (Wavemetrics). The ToF-ACSM was regularly calibrated (ionization efficiency), and relative ionization efficiency (RIE) of NH₄ (3.76) and SO₄ (0.88) was experimentally determined by using nebulizing aqueous solutions of pure NH₄NO₃ and pure (NH₄)₂SO₄ into the ToF-ACSM. Default relative ionization efficiency (RIE) values were used for organics (1.4), nitrate (1.1), and chloride (1.3). The organic mass spectra from the ToF-ACSM were analyzed by positive matrix factorization (PMF) to identify and quantify the potential sources of organic aerosol (OA). We solved the PMF by the multilinear engine (ME-2) algorithm implemented within the toolkit SoFi, Source Finder.³⁵ Exploratory unconstrained PMF runs separated primary OA (POA) from traffic (HOA), cooking (COA), a component representing residential heating (mixture of biomass burning, BBOA, and coal combustion, CCOA), and a component representing secondary OA (SOA).

MALTE-Box Model. Measured particle size distributions from the SMPS were used in the zero-dimensional model MALTE-box, which simulates atmospheric chemistry and aerosol dynamics.³⁶ Since the chemical structure and therefore the reaction rates of the measured OOM compounds were not known, the chemistry module in MALTE-box was bypassed, and the aerosol dynamics was applied using measured oxygenated organic molecules. To calculate the condensation and evaporation of the vapors to and from the particle phase, the model uses their molecular mass and saturation vapor pressure, calculated using a parametrization by Donahue et al. (2012) and experimentally confirmed by Wang et al. (2020). The evaporation and condensation are explicitly calculated for each gas compound and particle diameter using the Fuchs-Sutugin corrected collision rate and the Kelvin and Raoult's effect. Particle size evolution is then due to particle growth and coagulation.

To focus the simulations on the effect of the measured OOMs to the mass increase in the particle phase, the model was run in a constricted mode so that every 10 min the measured particle size distribution was used to initialize the model distribution. The measured OOMs were then allowed to condense to (or evaporate from) the particles, according to their saturation vapor pressures and concentrations. From the modeled output, the flux of the vapors to particle phase was calculated using the time in between the consecutive model initializations. In this way, we were able to use the measured

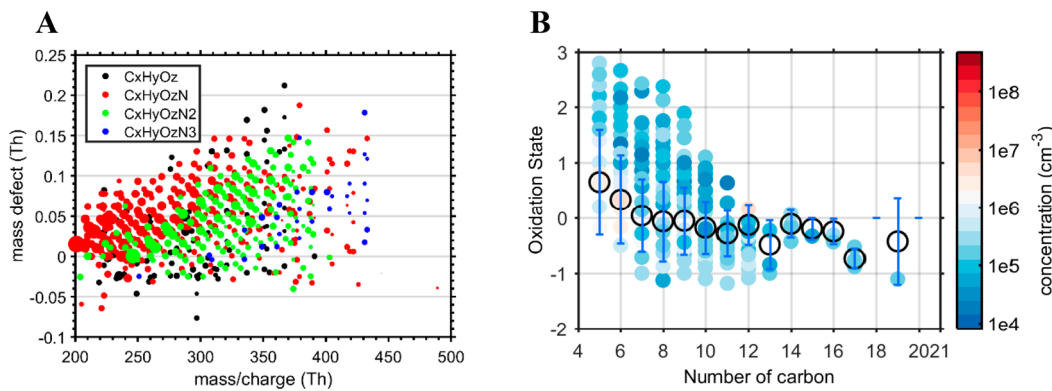


Figure 1. (a) Campaign averaged OOM mass defect versus m/z in Beijing. Mass defect is the difference between the exact mass and the nominal mass (the exact mass of ^1H is 1.007276 Da, giving a positive mass defect of 0.007276). Symbol size is proportional to the logarithm of the counting rate. Most species contain at least one N atom. (b) Campaign averaged carbon oxidation state as a function of carbon numbers. Black circles show mean values, with error bars showing the standard deviation. Symbol color corresponds to concentration.

conditions as closely as possible and assess the mass flux at any particular moment.

RESULTS AND DISCUSSION

Molecular Characterization of OOMs. In Figure 1(a,b), we present molecular characteristics of oxygenated organic molecules (OOMs) measured in Beijing by an NO_3 -Cl-APi-ToF; however, we cannot classify all of these OOMs as highly oxygenated organic molecules (HOMs).¹⁷ Most of these OOMs have molecular masses between 200 and 450 amu, with carbon numbers between 5 and 18. Molecules with one or two nitrogen atoms predominate, and the highest signals are from nitrophenol related compounds, e.g., $\text{C}_6\text{H}_5\text{NO}_3$ and $\text{C}_7\text{H}_7\text{NO}_3$. The measured total OOM concentration on average is around $1\text{--}2 \times 10^9$ molecules cm^{-3} , which is 10 times higher than the values measured in a boreal forest region dominated by monoterpene emissions.³⁷ The OOM concentrations are highest during haze periods (with $\text{PM}_{2.5} > 75 \mu\text{g m}^{-3}$), which may be explained by high concentrations of total aromatic volatile organic compounds (the summed concentrations of benzene, toluene, trimethylbenzene, ethyl toluene, propyl benzene, and diethylbenzene) as shown in Figure S1(b). To elucidate the evolution of OOMs and aromatic precursors, as well as nitrous acid (HONO), we show the diurnal variation of these parameters along with boundary layer height (see Figure S1). These compounds are largely mediated by boundary layer processes; high concentrations of OOMs, aromatic vapors, and organic aerosol usually occurred during nighttime with a shallow boundary layer.

In the urban atmosphere, OH and NO_3 are the dominant oxidants for most aromatic compounds; once the oxidants attack the aromatic ring, autoxidation can be triggered.^{16,24} However, high concentrations of NO in ambient Beijing can terminate autoxidation and lead to the formation of compounds containing multiple nitrogen atoms.^{26,27,38} Noting that these closed-shell products still are reactive with OH and NO_3 , multiple generations of oxidation may occur in the atmosphere as well as in chamber studies.²⁷ We observed compounds containing several nitrogen atoms in ambient Beijing, as depicted in Figure 1(a), consistent with both autoxidation and multigeneration chemistry.

Overall, the oxidation chemistry can be represented by the oxidation state of carbon.³⁹ As shown in Figure 1(b), the average oxidation state of carbon in the ambient vapors

measured with the NO_3 -Cl-APi-ToF tends to decrease with an increasing carbon number. The highest carbon oxidation state occurs in molecules with 5 carbons, with formulas $\text{C}_5\text{H}_9\text{NO}_6$ and $\text{C}_5\text{H}_{10}\text{N}_2\text{O}_8$, which are related to multigeneration oxidation products from isoprene terminated by NO (see data in Figure S3). Note that the source of isoprene and monoterpenes is not only biogenic emission but also emission of anthropogenic volatile chemical products.^{40,41} The carbon oxidation state presented here is higher than that in the boreal forest region, which is dominated by monoterpenes with lower NO_x concentrations.⁴² The conditions with high NO concentration and strong atmospheric oxidation capacity favoring multigeneration reactions lead to a high carbon oxidation state in Beijing, while first-generation products are the dominant products in the boreal forest region.²¹ This may be the main reason for the large discrepancy in the carbon oxidation state between the two environments.

The oxidized vapors we measure with the NO_3 -Cl-APi-ToF are a key bridge connecting aromatic precursors emitted in the urban atmosphere to oxygenated organic aerosol and thus haze formation. As shown in Figure 2(a), the variation of OOMs shows a good correlation with aromatic VOCs during both haze and clean periods (defined by a high or low condensation sink). Aromatic VOC emissions are predominately on-road

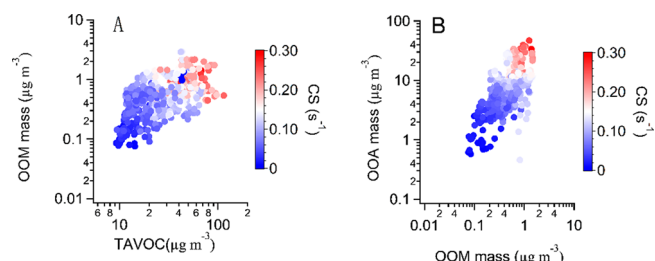


Figure 2. (a) Scatter plot of total OOM concentration vs total aromatic VOCs (TAVOCs) in Beijing during the measurement period. The symbol color indicates the aerosol condensation sink, which correlates with the aerosol pollution level and directly controls the sink of condensable organic vapors (OOMs). (b) Scatter plot of total OOM concentration vs oxygenated organic aerosol (OOA). OOA is a factor resolved by positive matrix factorization (PMF) of ambient organic aerosol measured by a ToF-ACSM. These associations are likely causal, with aromatic VOC oxidation driving OOM production and OOM condensation driving OOA formation.

vehicle exhaust.⁴⁰ The formation of secondary organic aerosol from anthropogenic VOCs has been the subject of numerous chamber studies. In general, long-chain alkanes and aromatic compounds (benzene, toluene, etc.) are considered to be the main precursors of anthropogenic SOA.⁴³ Given the large emission sources of anthropogenic VOCs and their fate in ambient Beijing, these aromatic VOCs should be a large source of the OOMs observed here.⁴⁴ OOM condensation may in turn be the main source of SOA. Figure 2(b) shows that there is a strong correlation between OOMs and the oxidized organic aerosol (OOA) factor measured by a time-of-flight aerosol chemical speciation monitor (ToF-ACSM), suggesting that condensation of these OOMs contributes to the mass of OOA. The OOA in turn constitutes the majority of the OA, especially during haze events.

Contributions of OOMs to PM and Haze. The relative contribution of different OOMs to SOA formation depends on their driving forces for net condensation, largely constrained by vapor concentration and volatility.^{10,45,46} We estimate the volatility of observed OOMs using a combination of two quantitatively confirmed VBS parametrizations to reflect the contribution of aging (multigeneration OH oxidation)^{45,46} and autoxidation¹⁷ to the OOM formation, respectively (see Figure S4).²⁶ Because the volatility of OOMs varies by more than 10 decades, we group them together within a volatility basis set (VBS) (Figure 3).

In general, OOMs during haze periods have a similar volatility distribution to that during nonhaze periods but with notably higher concentrations in all volatility bins (Figure 3A). The ultralow, extremely low, and low-volatility organic compounds (ULVOCs, ELVOCs, and LVOCs) have sufficiently low saturation vapor pressures to be efficient condensable material; the semivolatile organic compounds (SVOCs) contribute to particle mass via equilibrium gas-particle partitioning. Intermediate volatile organic compounds (IVOCs), however, have a minor direct contribution to SOA formation in this study, although the most abundant OOMs were phenolic compounds such as nitrophenol. We integrate OOMs from the lowest volatility bin to $C^* \leq 10^{0.5} \mu\text{g m}^{-3}$, to show the tentative abundance of condensable vapors (shaded area in Figure 3B). OOMs potentially formed from the aging pathway and the autoxidation pathway are separated by a dashed dividing line (Figure 3B and Figure S4). Interestingly, during both the haze and nonhaze periods, the aging products dominate in the ULVOC range, while the autoxidation products become more abundant in the ELVOC range and take over in the LVOC range. The overall increase in the tentative condensable vapors from nonhaze to haze periods is approximately 40% in mass (Figure 3C). Moreover, the OOMs in the ULVOC and ELVOC ranges rise more than those in the LVOC range, with species potentially formed from aging pathways being the major contributor. This suggests that photochemical aging might be a major process that drives the SOA formation we observe in Beijing during the observation periods.

To quantify the contribution of the measured OOMs to the mass concentration of organic aerosol in $\text{PM}_{2.5}$, we estimated the contribution of OOMs to the total $\text{PM}_{2.5}$ mass flux using MALTE-box (Model to predict Aerosol formation in Lower Troposphere, see Materials and Methods), which treats both gas-to-particle condensation and evaporation of OOMs from particles. We restricted our analysis to periods of $\text{PM}_{2.5}$ growth so that we could constrain the mass flux via the measured

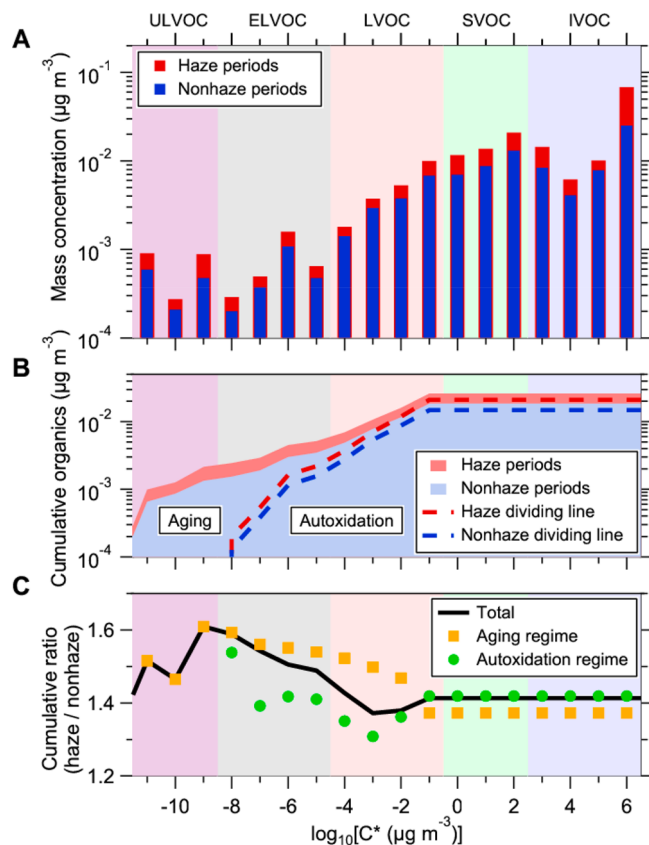
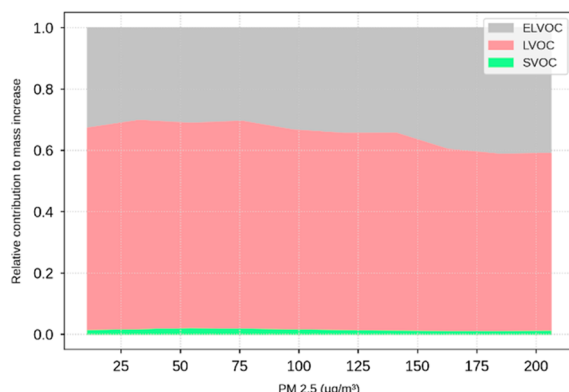


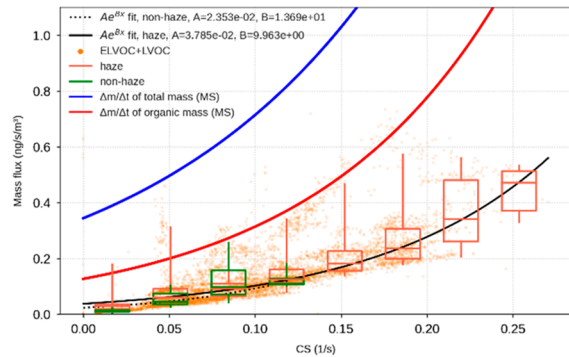
Figure 3. (a) The summed OOM concentrations in each bin of the volatility basis set during haze (red) and nonhaze (blue) periods. The ULVOCs, ELVOCs, and LVOCs have sufficiently low volatilities and are efficient condensable material; the SVOCs contribute to particle mass via gas-particle partitioning. (b) The cumulative OOM concentrations. The OOMs are integrated from the lowest volatility bin to $C^* \leq 10^{0.5} \mu\text{g m}^{-3}$ (shaded area), indicating the tentative abundance of condensable vapors. The dashed dividing lines show volatilities estimated using two distinct VBS parametrizations to reflect the contribution of aging (multigeneration OH oxidation) and autoxidation to the OOM formation, respectively (see Materials and Methods and Figure S5). (c) The ratio of cumulative OOM concentrations during haze periods to those during nonhaze periods. The solid black line, yellow squares, and green circles represent the ratio of total OOMs, OOMs in the aging regime, and OOMs in the autoxidation regime, respectively. OOMs during haze periods have a similar volatility distribution to that during nonhaze periods but with notably higher concentrations in all volatility bins. The overall increase in the tentative condensable vapors from nonhaze to haze periods is approximately 40% in mass. Further, these OOMs in the ULVOC and ELVOC ranges rise more than those in the LVOC range, with species potentially formed from aging pathways being the major contributor.

growth rate. As shown in Figure 4(a), LVOCs and ELVOCs dominated aerosol mass growth, consistent with being saturated as observed. Overall, 26% and 39% of the organic aerosol mass increase are explained by condensation of OOMs during nonhaze and haze conditions, respectively (see Figure 4c). This corresponds to 9% and 23% of the total $\text{PM}_{2.5}$ mass increase. The uncertainties of these values due to uncertain volatility are limited, as shown in Table S1. The additional organic growth implied by the difference between the measured (ToF-ACSM) organic mass growth and the calculated OOM condensation rate is likely due to some combination of aqueous condensed-phase chemistry and

A



B



C

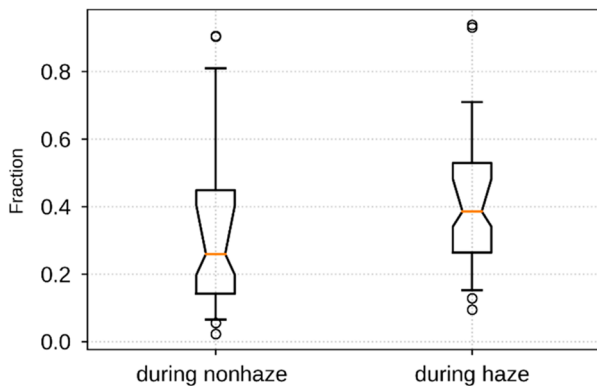


Figure 4. (a) The relative contributions of ELVOCs, LVOCs, and SVOCs to modeled total mass flux for different PM_{2.5} levels, noting that ULVOCs are also included in ELVOCs during the modeling. Contributions are based on growth rates modeled during growth periods and measured vapor concentrations. (b) The variation of total mass fluxes of ELVOCs and LVOCs as a function of condensation sink (CS). The black solid curve and red box and whisker ranges are for PM_{2.5} > 75 µg m⁻³ (haze periods), while the dotted curve and green box and whisker ranges are for PM_{2.5} < 75 µg m⁻³. The orange points represent total flux from ELVOCs and LVOCs. The blue and red solid curves represent modeled total mass fluxes and organic mass fluxes during positive mass flux events. (c) The contribution of OOMs to organic aerosol mass during nonhaze and haze periods. The organic aerosol mass in PM_{2.5} mass is measured by a ToF-ACSM, along with nitrate, sulfate, ammonium, and chloride.

equilibrium partitioning of unmeasured SVOCs, where the nitrate CI-API-ToF is less sensitive.⁴⁷ As listed in Table S2, the compounds with the largest contributions to the flux were

C₁₀H₁₄O₉N, C₁₀H₁₅O₈N, and C₁₀H₁₆O₉N₂, which may arise from monoterpane oxidation, and C₁₄H₁₅O₈N, C₁₂H₂₀O₈N₂, and C₈H₁₃O₁₁, which may arise from aromatic oxidation. Most of the mass flux is driven by numerous products likely associated with a variety of aromatic precursors.

The higher contribution of OOMs to PM_{2.5} and organic aerosol mass during the haze periods is associated with a higher condensation sink and higher OOM concentrations, which may enhance the gas-to-particle conversion. As we show in Figure 4(b), the empirical relationship between mass fluxes and condensation sink is nonlinear, indicating enhanced vapor condensation to pre-existing aerosol as haze grows more severe.

Although our study provides a quantified relationship between oxygenated organic vapor molecules in the gas phase and organic aerosol in the particle phase, uncertainties and limitations still exist. First, we quantify all OOMs based on the sulfuric acid calibration, but the binding affinity of the nitrate anion to organic functional groups may vary, adding uncertainty. However, for many highly functionalized OOMs, the same kinetic limit that applies to sulfuric acid is likely to hold. Second, we estimate volatility based on measured molecular composition rather than measuring the exact vapor pressure of individual OOM species. Therefore, the parametrized volatility distribution will lead to uncertainty in estimated partitioning. However, the measured volatility of aromatic oxidation products matches this parametrization to within a factor of 10.²⁶ Finally, advection and external sources and sinks are not explicitly considered in the box model, and a fraction of organic aerosol in the urban atmosphere is from transport of the upwind region, with aging processes occurring within the plume, while the formation of OOM vapors is likely to be local.

Quantification of specific chemical oxidation products from various organic precursors and their contribution to SOA formation during haze episodes is essential to understand haze formation. Those molecular formation mechanisms of SOA, and thereby haze, are far from being completely elucidated in megacities like Beijing. Our results reveal a substantial pool of oxygenated organic vapors that can condense to particles and explain 26–39% of organic aerosol mass growth. We show that most of these OOMs are nitrogen containing compounds, suggesting that multistep oxidation processes are essential in the urban atmosphere. In particular, these OOMs contribute more during high PM loading conditions, due to both increased OOM concentrations and condensation sink, which facilitates gas-to-particle conversion processes. Noting that the nitrate chemical ionization scheme is only sensitive to a subset of compounds, e.g., organic molecules with –OOH groups, –OH groups, and/or –NO₂ groups, other quantitative chemical ionization methods should be employed to develop a comprehensive picture of oxygenated volatile organic compounds. Regardless, our current results could provide a substantial number of oxygenated VOCs for air quality models that are currently not treated.

ASSOCIATED CONTENT

Supporting Information

The Supporting Information is available free of charge at <https://pubs.acs.org/doi/10.1021/acs.est.1c05191>.

Details on measurement of VOCs and HONO; data sources of NO₂, O₃, SO₂, and PM_{2.5}; measurement of

mixing layer height; calculation method of condensation sink; estimation of volatility of OOMs; Figure S1, time series of organic aerosol factors; Figure 2, variation of mixing layer height, PM_{2.5} mass concentration; Figure S3, possible formation pathway of C₅H₁₀N₂O₈ and C₅H₉NO₆; Figure S4, Van Krevelen diagram; Figure S5, variation of total modeled mass flux as functions of ELVOCs, LVOCs, and SVOCs (condensation sink); Figure S6, variation of total modeled mass flux as functions of ELVOCs, LVOCs, and SVOCs (relative humidity); Table S1, statistics of OOM contribution; and Table S2, OOM with largest contributions to aerosol mass growth ([PDF](#))

AUTHOR INFORMATION

Corresponding Authors

Markku Kulmala — *Aerosol and Haze Laboratory, Beijing Advanced Innovation Center for Soft Matter Science and Engineering, Beijing University of Chemical Technology, Beijing 100089, China; Institute for Atmospheric and Earth System Research/Physics, Faculty of Science, University of Helsinki, Helsinki 00560, Finland;*
Email: markku.kulmala@helsinki.fi

Yongchun Liu — *Aerosol and Haze Laboratory, Beijing Advanced Innovation Center for Soft Matter Science and Engineering, Beijing University of Chemical Technology, Beijing 100089, China; Email: liuyc@buct.edu.cn*

Jingkun Jiang — *School of Environment, Tsinghua University, Beijing 100084, China; Email: jiangjk@tsinghua.edu.cn*

Yonghong Wang — *Aerosol and Haze Laboratory, Beijing Advanced Innovation Center for Soft Matter Science and Engineering, Beijing University of Chemical Technology, Beijing 100089, China; Institute for Atmospheric and Earth System Research/Physics, Faculty of Science, University of Helsinki, Helsinki 00560, Finland; Research Center for Eco-Environmental Sciences, Chinese Academy of Sciences, Beijing 100085, China; [orcid.org/0000-0003-2498-9143](#); Email: yonghongwang@rcees.ac.cn*

Authors

Petri Clusius — *Institute for Atmospheric and Earth System Research/Physics, Faculty of Science, University of Helsinki, Helsinki 00560, Finland*

Chao Yan — *Institute for Atmospheric and Earth System Research/Physics, Faculty of Science, University of Helsinki, Helsinki 00560, Finland*

Kaspar Dällenbach — *Institute for Atmospheric and Earth System Research/Physics, Faculty of Science, University of Helsinki, Helsinki 00560, Finland*

Ruijing Yin — *School of Environment, Tsinghua University, Beijing 100084, China*

Mingyi Wang — *Center for Atmospheric Particle Studies, Carnegie Mellon University, Pittsburgh, Pennsylvania 15213, United States; [orcid.org/0000-0001-5782-2513](#)*

Xu-Cheng He — *Institute for Atmospheric and Earth System Research/Physics, Faculty of Science, University of Helsinki, Helsinki 00560, Finland; [orcid.org/0000-0002-7416-306X](#)*

Biwu Chu — *Research Center for Eco-Environmental Sciences, Chinese Academy of Sciences, Beijing 100085, China; [orcid.org/0000-0002-7548-5669](#)*

Yiqun Lu — *Department of Environmental Science & Engineering, Fudan University, Shanghai 200438, China*

Lubna Dada — *Institute for Atmospheric and Earth System Research/Physics, Faculty of Science, University of Helsinki, Helsinki 00560, Finland*

Juha Kangasluoma — *Aerosol and Haze Laboratory, Beijing Advanced Innovation Center for Soft Matter Science and Engineering, Beijing University of Chemical Technology, Beijing 100089, China; Institute for Atmospheric and Earth System Research/Physics, Faculty of Science, University of Helsinki, Helsinki 00560, Finland; [orcid.org/0000-0002-1639-1187](#)*

Pekka Rantala — *Institute for Atmospheric and Earth System Research/Physics, Faculty of Science, University of Helsinki, Helsinki 00560, Finland*

Chenjuan Deng — *School of Environment, Tsinghua University, Beijing 100084, China*

Zhuohui Lin — *Aerosol and Haze Laboratory, Beijing Advanced Innovation Center for Soft Matter Science and Engineering, Beijing University of Chemical Technology, Beijing 100089, China*

Weigang Wang — *Institute of Chemistry, Chinese Academy of Sciences, Beijing 100029, China; [orcid.org/0000-0001-6911-1110](#)*

Lei Yao — *Institute for Atmospheric and Earth System Research/Physics, Faculty of Science, University of Helsinki, Helsinki 00560, Finland; [orcid.org/0000-0002-2680-1629](#)*

Xiaolong Fan — *Aerosol and Haze Laboratory, Beijing Advanced Innovation Center for Soft Matter Science and Engineering, Beijing University of Chemical Technology, Beijing 100089, China*

Wei Du — *Institute for Atmospheric and Earth System Research/Physics, Faculty of Science, University of Helsinki, Helsinki 00560, Finland*

Jing Cai — *Institute for Atmospheric and Earth System Research/Physics, Faculty of Science, University of Helsinki, Helsinki 00560, Finland*

Liine Heikkinen — *Institute for Atmospheric and Earth System Research/Physics, Faculty of Science, University of Helsinki, Helsinki 00560, Finland*

Yee Jun Tham — *Institute for Atmospheric and Earth System Research/Physics, Faculty of Science, University of Helsinki, Helsinki 00560, Finland*

Qiaozhi Zha — *Institute for Atmospheric and Earth System Research/Physics, Faculty of Science, University of Helsinki, Helsinki 00560, Finland*

Zhenhao Ling — *Institute for Atmospheric and Earth System Research/Physics, Faculty of Science, University of Helsinki, Helsinki 00560, Finland*

Heikki Junninen — *Institute for Atmospheric and Earth System Research/Physics, Faculty of Science, University of Helsinki, Helsinki 00560, Finland; Institute of Physics, University of Tartu, Tartu 50090, Estonia*

Tuukka Petäjä — *Institute for Atmospheric and Earth System Research/Physics, Faculty of Science, University of Helsinki, Helsinki 00560, Finland*

Maofa Ge — *Institute of Chemistry, Chinese Academy of Sciences, Beijing 100029, China; [orcid.org/0000-0002-1771-9359](#)*

Yuesi Wang — *Institute of Atmospheric Physics, Chinese Academy of Sciences, Beijing 100029, China*

Hong He — *Research Center for Eco-Environmental Sciences, Chinese Academy of Sciences, Beijing 100085, China; [orcid.org/0000-0001-8476-8217](#)*

- Douglas R. Worsnop — Aerodyne Research Inc., Billerica, Massachusetts 01821, United States
- Veli-Matti Kerminen — Institute for Atmospheric and Earth System Research/Physics, Faculty of Science, University of Helsinki, Helsinki 00560, Finland
- Federico Bianchi — Aerosol and Haze Laboratory, Beijing Advanced Innovation Center for Soft Matter Science and Engineering, Beijing University of Chemical Technology, Beijing 100089, China; Institute for Atmospheric and Earth System Research/Physics, Faculty of Science, University of Helsinki, Helsinki 00560, Finland; orcid.org/0000-0003-2996-3604
- Lin Wang — Department of Environmental Science & Engineering, Fudan University, Shanghai 200438, China; orcid.org/0000-0002-4905-3432
- Michael Boy — Institute for Atmospheric and Earth System Research/Physics, Faculty of Science, University of Helsinki, Helsinki 00560, Finland
- Mikael Ehn — Institute for Atmospheric and Earth System Research/Physics, Faculty of Science, University of Helsinki, Helsinki 00560, Finland; orcid.org/0000-0002-0215-4893
- Neil M. Donahue — Center for Atmospheric Particle Studies, Carnegie Mellon University, Pittsburgh, Pennsylvania 15213, United States; orcid.org/0000-0003-3054-2364

Complete contact information is available at:
<https://pubs.acs.org/10.1021/acs.est.1c05191>

Author Contributions

Y.W. designed the research. Y.W., C.Y., K.D., R.Y., X.H., B.C., J.K., P.R., C.D., W.W., L.H., H.J., F.B., L.W., J.J., and Y.L. conducted the measurements. P.C. and M.B. performed box model simulation. Y.W., L.D., Z.L., L.Y., X.F., W.D., J.C., Y.T., T.P., M.G., Y.W., H.H., D.W., V.K., M.E., and N.D. contributed to the scientific discussions. Y.W. wrote the main manuscript with contributions from N.D., M.W., and P.C.

Notes

The authors declare no competing financial interest.

Data and Materials Availability. Data and materials are available upon contacting the corresponding authors.

ACKNOWLEDGMENTS

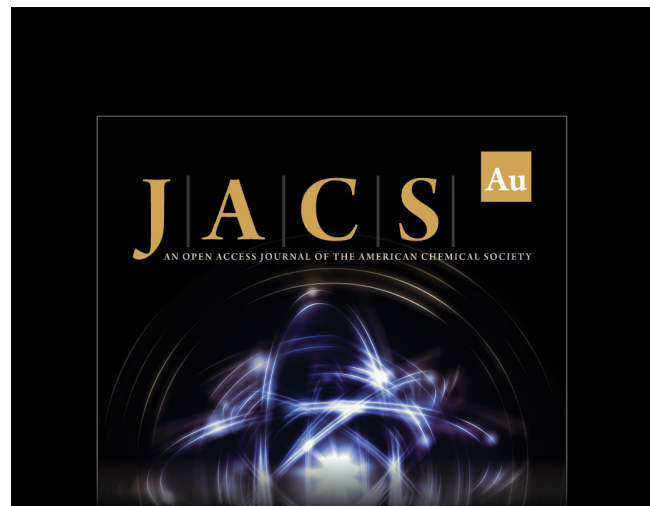
This work was supported by funding from the Beijing University of Chemical Technology, the National Natural Science Foundation of China (41877306), the European Research Council via advanced grant ATM-GTP (project no. 742206), and the Academy of Finland via the Academy professor project of M.K. N.M.D. acknowledges the following support: US NSF CHE-1807530. K.R.D. acknowledges support from the Swiss National Science Foundation mobility grant P2EZP2_181599. H.J. acknowledges support from the European Regional Development Fund (project no. MOBTT42).

REFERENCES

- (1) Lelieveld, J.; Evans, J. S.; Fnais, M.; Giannadaki, D.; Pozzer, A. The contribution of outdoor air pollution sources to premature mortality on a global scale. *Nature* **2015**, *525*, 367.
- (2) Ding, A. J.; Huang, X.; Nie, W.; Sun, J. N.; Kerminen, V. M.; Petäjä, T.; Su, H.; Cheng, Y. F.; Yang, X. Q.; Wang, M. H.; Chi, X. G.; Wang, J. P.; Virkkula, A.; Guo, W. D.; Yuan, J.; Wang, S. Y.; Zhang, R. J.; Wu, Y. F.; Song, Y.; Zhu, T.; Zilitinkevich, S.; Kulmala, M.; Fu, C. B. Enhanced haze pollution by black carbon in megacities in China. *Geophys. Res. Lett.* **2016**, *43* (6), 2873–2879.
- (3) Zhang, Q.; Jiang, X.; Tong, D.; Davis, S. J.; Zhao, H.; Geng, G.; Feng, T.; Zheng, B.; Lu, Z.; Streets, D. G.; Ni, R.; Brauer, M.; van Donkelaar, A.; Martin, R. V.; Huo, H.; Liu, Z.; Pan, D.; Kan, H.; Yan, Y.; Lin, J.; He, K.; Guan, D. Transboundary health impacts of transported global air pollution and international trade. *Nature* **2017**, *543* (7647), 705–709.
- (4) An, Z.; Huang, R. J.; Zhang, R.; Tie, X.; Li, G.; Cao, J.; Zhou, W.; Shi, Z.; Han, Y.; Gu, Z.; Ji, Y. Severe haze in northern China: A synergy of anthropogenic emissions and atmospheric processes. *Proc. Natl. Acad. Sci. U. S. A.* **2019**, *116* (18), 8657–8666.
- (5) Zhang, Q.; Zheng, Y.; Tong, D.; Shao, M.; Wang, S.; Zhang, Y.; Xu, X.; Wang, J.; He, H.; Liu, W.; Ding, Y.; Lei, Y.; Li, J.; Wang, Z.; Zhang, X.; Wang, Y.; Cheng, J.; Liu, Y.; Shi, Q.; Yan, L.; Geng, G.; Hong, C.; Li, M.; Liu, F.; Zheng, B.; Cao, J.; Ding, A.; Gao, J.; Fu, Q.; Huo, J.; Liu, B.; Liu, Z.; Yang, F.; He, K.; Hao, J. Drivers of improved PM_{2.5} air quality in China from 2013 to 2017. *Proc. Natl. Acad. Sci. U. S. A.* **2019**, *116* (49), 24463–24469.
- (6) Wang, Y.; Gao, W.; Wang, S.; Song, T.; Gong, Z.; Ji, D.; Wang, L.; Liu, Z.; Tang, G.; Huo, Y.; Tian, S.; Li, J.; Li, M.; Yang, Y.; Chu, B.; Petäjä, T.; Kerminen, V.-M.; He, H.; Hao, J.; Kulmala, M.; Wang, Y.; Zhang, Y. Contrasting trends of PM_{2.5} and surface-ozone concentrations in China from 2013 to 2017. *National Science Review* **2020**, *7* (8), 1331–1339.
- (7) Huang, R. J.; Zhang, Y.; Bozzetti, C.; Ho, K. F.; Cao, J. J.; Han, Y.; Daellenbach, K. R.; Slowik, J. G.; Platt, S. M.; Canonaco, F.; Zotter, P.; Wolf, R.; Pieber, S. M.; Bruns, E. A.; Crippa, M.; Ciarelli, G.; Piazzalunga, A.; Schwikowski, M.; Abbaszade, G.; Schnelle-Kreis, J.; Zimmermann, R.; An, Z.; Szidat, S.; Baltensperger, U.; El Haddad, I.; Prevot, A. S. High secondary aerosol contribution to particulate pollution during haze events in China. *Nature* **2014**, *514* (7521), 218–222.
- (8) Hallquist, M.; Wenger, J. C.; Baltensperger, U.; Rudich, Y.; Simpson, D.; Claeys, M.; Dommen, J.; Donahue, N. M.; George, C.; Goldstein, A. H.; Hamilton, J. F.; Herrmann, H.; Hoffmann, T.; Iinuma, Y.; Jang, M.; Jenkin, M. E.; Jimenez, J. L.; Kiendler-Scharr, A.; Maenhaut, W.; McFiggans, G.; Mentel, T. F.; Monod, A.; Prévôt, A. S. H.; Seinfeld, J. H.; Surratt, J. D.; Szmigielski, R.; Wildt, J. The formation, properties and impact of secondary organic aerosol: current and emerging issues. *Atmos. Chem. Phys.* **2009**, *9* (14), 5155–5236.
- (9) Jimenez, J. L.; Canagaratna, M. R.; Donahue, N. M.; Prevot, A. S. H.; Zhang, Q.; Kroll, J. H.; DeCarlo, P. F.; Allan, J. D.; Coe, H.; Ng, N. L.; Aiken, A. C.; Docherty, K. S.; Ulbrich, I. M.; Grieshop, A. P.; Robinson, A. L.; Duplissy, J.; Smith, J. D.; Wilson, K. R.; Lanz, V. A.; Hueglin, C.; Sun, Y. L.; Tian, J.; Laaksonen, A.; Raatikainen, T.; Rautiainen, J.; Vaattovaara, P.; Ehn, M.; Kulmala, M.; Tomlinson, J. M.; Collins, D. R.; Cubison, M. J.; Dunlea, J.; Huffman, J. A.; Onasch, T. B.; Alfarra, M. R.; Williams, P. I.; Bower, K.; Kondo, Y.; Schneider, J.; Drewnick, F.; Borrmann, S.; Weimer, S.; Demerjian, K.; Salcedo, D.; Cottrell, L.; Griffin, R.; Takami, A.; Miyoshi, T.; Hatakeyama, S.; Shimono, A.; Sun, J. Y.; Zhang, Y. M.; Dzepina, K.; Kimmel, J. R.; Sueper, D.; Jayne, J. T.; Herndon, S. C.; Trimborn, A. M.; Williams, L. R.; Wood, E. C.; Middlebrook, A. M.; Kolb, C. E.; Baltensperger, U.; Worsnop, D. R. Evolution of Organic Aerosols in the Atmosphere. *Science* **2009**, *326* (5959), 1525–1529.
- (10) Riipinen, I.; Yli-Juuti, T.; Pierce, J. R.; Petäjä, T.; Worsnop, D. R.; Kulmala, M.; Donahue, N. M. The contribution of organics to atmospheric nanoparticle growth. *Nat. Geosci.* **2012**, *5* (7), 453–458.
- (11) Ervens, B.; Turpin, B. J.; Weber, R. J. Secondary organic aerosol formation in cloud droplets and aqueous particles (aqSOA): a review of laboratory, field and model studies. *Atmos. Chem. Phys.* **2011**, *11* (21), 11069–11102.
- (12) Gkatzelis, G. I.; Papanastasiou, D. K.; Karydis, V. A.; Hohaus, T.; Liu, Y.; Schmitt, S. H.; Schlag, P.; Fuchs, H.; Novelli, A.; Chen, Q.; Cheng, X.; Broch, S.; Dong, H.; Holland, F.; Li, X.; Liu, Y.; Ma, X.; Reimer, D.; Rohrer, F.; Shao, M.; Tan, Z.; Taraborrelli, D.; Tillmann, R.; Wang, H.; Wang, Y.; Wu, Y.; Wu, Z.; Zeng, L.; Zheng,

- J.; Hu, M.; Lu, K.; Hofzumahaus, A.; Zhang, Y.; Wahner, A.; Kiendler-Scharr, A. Uptake of Water-soluble Gas-phase Oxidation Products Drives Organic Particulate Pollution in Beijing. *Geophys. Res. Lett.* **2021**, *48* (8), e2020GL091351.
- (13) Huang, R.-J.; Zhang, Y.; Bozzetti, C.; Ho, K. F.; Cao, J.; Han, Y.; Daellenbach, K.; G Slowik, J.; Platt, S.; Canonaco, F.; Zotter, P.; Wolf, R.; Pieber, S.; Bruns, E.; Crippa, M.; Ciarelli, G.; Piazzalunga, A.; Schwikowski, M.; Abbaszade, G.; Prevot, A. High secondary aerosol contribution to particulate pollution during haze events in China. *Nature* **2014**, *514*, 218.
- (14) Guo, S.; Hu, M.; Zamora, M. L.; Peng, J.; Shang, D.; Zheng, J.; Du, Z.; Wu, Z.; Shao, M.; Zeng, L.; Molina, M. J.; Zhang, R. Elucidating severe urban haze formation in China. *Proc. Natl. Acad. Sci. U. S. A.* **2014**, *111* (49), 17373–8.
- (15) Sun, Y.; Jiang, Q.; Wang, Z.; Fu, P.; Li, J.; Yang, T.; Yin, Y. Investigation of the sources and evolution processes of severe haze pollution in Beijing in January 2013. *Journal of Geophysical Research: Atmospheres* **2014**, *119* (7), 4380–4398.
- (16) Atkinson, R.; Arey, J. Atmospheric Degradation of Volatile Organic Compounds. *Chem. Rev.* **2003**, *103* (12), 4605–4638.
- (17) Bianchi, F.; Kurten, T.; Riva, M.; Mohr, C.; Rissanen, M. P.; Roldin, P.; Berndt, T.; Crounse, J. D.; Wennberg, P. O.; Mentel, T. F.; Wildt, J.; Junninen, H.; Jokinen, T.; Kulmala, M.; Worsnop, D. R.; Thornton, J. A.; Donahue, N.; Kjaergaard, H. G.; Ehn, M. Highly Oxygenated Organic Molecules (HOM) from Gas-Phase Autoxidation Involving Peroxy Radicals: A Key Contributor to Atmospheric Aerosol. *Chem. Rev.* **2019**, *119* (6), 3472–3509.
- (18) Zhang, R.; Wang, G.; Guo, S.; Zamora, M. L.; Ying, Q.; Lin, Y.; Wang, W.; Hu, M.; Wang, Y. Formation of Urban Fine Particulate Matter. *Chem. Rev.* **2015**, *115* (10), 3803–3855.
- (19) Donahue, N. M.; Ortega, I. K.; Chuang, W.; Riipinen, I.; Riccobono, F.; Schobesberger, S.; Dommen, J.; Baltensperger, U.; Kulmala, M.; Worsnop, D. R.; Vehkamaki, H. How do organic vapors contribute to new-particle formation? *Faraday Discuss.* **2013**, *165*, 91–104.
- (20) Trostl, J.; Chuang, W. K.; Gordon, H.; Heinritzi, M.; Yan, C.; Molteni, U.; Ahlm, L.; Frege, C.; Bianchi, F.; Wagner, R.; Simon, M.; Lehtipalo, K.; Williamson, C.; Craven, J. S.; Duplissy, J.; Adamov, A.; Almeida, J.; Bernhammer, A. K.; Breitenlechner, M.; Brilke, S.; Dias, A.; Ehrhart, S.; Flagan, R. C.; Franchin, A.; Fuchs, C.; Guida, R.; Gysel, M.; Hansel, A.; Hoyle, C. R.; Jokinen, T.; Junninen, H.; Kangasluoma, J.; Keskinen, H.; Kim, J.; Krapf, M.; Kurten, A.; Laaksonen, A.; Lawler, M.; Leiminger, M.; Mathot, S.; Mohler, O.; Nieminen, T.; Onnela, A.; Petaja, T.; Piel, F. M.; Miettinen, P.; Rissanen, M. P.; Rondo, L.; Sarnela, N.; Schobesberger, S.; Sengupta, K.; Sipila, M.; Smith, J. N.; Steiner, G.; Tome, A.; Virtanen, A.; Wagner, A. C.; Weingartner, E.; Wimmer, D.; Winkler, P. M.; Ye, P.; Carslaw, K. S.; Curtius, J.; Dommen, J.; Kirkby, J.; Kulmala, M.; Riipinen, I.; Worsnop, D. R.; Donahue, N. M.; Baltensperger, U. The role of low-volatility organic compounds in initial particle growth in the atmosphere. *Nature* **2016**, *533* (7604), 527–31.
- (21) Ehn, M.; Thornton, J. A.; Kleist, E.; Sipila, M.; Junninen, H.; Pullinen, I.; Springer, M.; Rubach, F.; Tillmann, R.; Lee, B.; Lopez-Hilfiker, F.; Andres, S.; Acir, I. H.; Rissanen, M.; Jokinen, T.; Schobesberger, S.; Kangasluoma, J.; Kontkanen, J.; Nieminen, T.; Kurten, T.; Nielsen, L. B.; Jorgensen, S.; Kjaergaard, H. G.; Canagaratna, M.; Maso, M. D.; Berndt, T.; Petaja, T.; Wahner, A.; Kerminen, V. M.; Kulmala, M.; Worsnop, D. R.; Wildt, J.; Mentel, T. F. A large source of low-volatility secondary organic aerosol. *Nature* **2014**, *506* (7489), 476–9.
- (22) Jokinen, T.; Sipila, M.; Richters, S.; Kerminen, V. M.; Paasonen, P.; Stratmann, F.; Worsnop, D.; Kulmala, M.; Ehn, M.; Herrmann, H.; Berndt, T. Rapid autoxidation forms highly oxidized RO₂ radicals in the atmosphere. *Angew. Chem., Int. Ed.* **2014**, *53* (52), 14596–600.
- (23) Mentel, T. F.; Springer, M.; Ehn, M.; Kleist, E.; Pullinen, I.; Kurtén, T.; Rissanen, M.; Wahner, A.; Wildt, J. Formation of highly oxidized multifunctional compounds: autoxidation of peroxy radicals formed in the ozonolysis of alkenes – deduced from structure–product relationships. *Atmos. Chem. Phys.* **2015**, *15* (12), 6745–6765.
- (24) Crounse, J. D.; Nielsen, L. B.; Jørgensen, S.; Kjaergaard, H. G.; Wennberg, P. O. Autoxidation of Organic Compounds in the Atmosphere. *J. Phys. Chem. Lett.* **2013**, *4* (20), 3513–3520.
- (25) Praske, E.; Otkjær, R. V.; Crounse, J. D.; Hethcox, J. C.; Stoltz, B. M.; Kjaergaard, H. G.; Wennberg, P. O. Atmospheric autoxidation is increasingly important in urban and suburban North America. *Proc. Natl. Acad. Sci. U. S. A.* **2018**, *115* (1), 64.
- (26) Wang, M.; Chen, D.; Xiao, M.; Ye, Q.; Stolzenburg, D.; Hofbauer, V.; Ye, P.; Vogel, A. L.; Mauldin, R. L., 3rd; Amorim, A.; Baccarini, A.; Baumgartner, B.; Brilke, S.; Dada, L.; Dias, A.; Duplissy, J.; Finkenzeller, H.; Garmash, O.; He, X. C.; Hoyle, C. R.; Kim, C.; Kvashnin, A.; Lehtipalo, K.; Fischer, L.; Molteni, U.; Petaja, T.; Pospisilova, V.; Quelever, L. L. J.; Rissanen, M.; Simon, M.; Tauber, C.; Tome, A.; Wagner, A. C.; Weitz, L.; Volkamer, R.; Winkler, P. M.; Kirkby, J.; Worsnop, D. R.; Kulmala, M.; Baltensperger, U.; Dommen, J.; El-Haddad, I.; Donahue, N. M. Photo-oxidation of Aromatic Hydrocarbons Produces Low-Volatility Organic Compounds. *Environ. Sci. Technol.* **2020**, *54* (13), 7911–7921.
- (27) Garmash, O.; Rissanen, M. P.; Pullinen, I.; Schmitt, S.; Kausiala, O.; Tillmann, R.; Zhao, D.; Percival, C.; Bannan, T. J.; Priestley, M.; Hallquist, Å. M.; Kleist, E.; Kiendler-Scharr, A.; Hallquist, M.; Berndt, T.; McFiggans, G.; Wildt, J.; Mentel, T. F.; Ehn, M. Multi-generation OH oxidation as a source for highly oxygenated organic molecules from aromatics. *Atmos. Chem. Phys.* **2020**, *20* (1), 515–537.
- (28) Jokinen, T.; Sipilä, M.; Junninen, H.; Ehn, M.; Lönn, G.; Hakala, J.; Petäjä, T.; Mauldin, R. L.; Kulmala, M.; Worsnop, D. R. Atmospheric sulphuric acid and neutral cluster measurements using CI-API-TOF. *Atmos. Chem. Phys.* **2012**, *12* (9), 4117–4125.
- (29) Yao, L.; Garmash, O.; Bianchi, F.; Zheng, J.; Yan, C.; Kontkanen, J.; Junninen, H.; Mazon, S. B.; Ehn, M.; Paasonen, P.; Sipilä, M.; Wang, M.; Wang, X.; Xiao, S.; Chen, H.; Lu, Y.; Zhang, B.; Wang, D.; Fu, Q.; Geng, F.; Li, L.; Wang, H.; Qiao, L.; Yang, X.; Chen, J.; Kerminen, V.-M.; Petäjä, T.; Worsnop, D. R.; Kulmala, M.; Wang, L. Atmospheric new particle formation from sulfuric acid and amines in a Chinese megacity. *Science* **2018**, *361* (6399), 278–281.
- (30) Brean, J.; Harrison, R. M.; Shi, Z.; Beddows, D. C. S.; Acton, W. J. F.; Hewitt, C. N.; Squires, F. A.; Lee, J. Observations of highly oxidized molecules and particle nucleation in the atmosphere of Beijing. *Atmos. Chem. Phys.* **2019**, *19* (23), 14933–14947.
- (31) Yan, C.; Yin, R.; Lu, Y.; Dada, L.; Yang, D.; Fu, Y.; Kontkanen, J.; Deng, C.; Garmash, O.; Ruan, J.; Baalbaki, R.; Schervish, M.; Cai, R.; Bloss, M.; Chan, T.; Chen, T.; Chen, Q.; Chen, X.; Chen, Y.; Chu, B.; Dällenbach, K.; Foreback, B.; He, X.; Heikkilä, L.; Jokinen, T.; Junninen, H.; Kangasluoma, J.; Kokkonen, T.; Kurppa, M.; Lehtipalo, K.; Li, H.; Li, H.; Li, X.; Liu, Y.; Ma, Q.; Paasonen, P.; Rantala, P.; Pileci, R. E.; Rusanen, A.; Sarnela, N.; Simonen, P.; Wang, S.; Wang, W.; Wang, Y.; Xue, M.; Yang, G.; Yao, L.; Zhou, Y.; Kujansuu, J.; Petäjä, T.; Nie, W.; Ma, Y.; Ge, M.; He, H.; Donahue, N. M.; Worsnop, D. R.; Veli-Matti, K.; Wang, L.; Liu, Y.; Zheng, J.; Kulmala, M.; Jiang, J.; Bianchi, F. The Synergistic Role of Sulfuric Acid, Bases, and Oxidized Organics Governing New-Particle Formation in Beijing. *Geophys. Res. Lett.* **2021**, *48* (7), e2020GL091944.
- (32) Li, Y. J.; Sun, Y.; Zhang, Q.; Li, X.; Li, M.; Zhou, Z.; Chan, C. K. Real-time chemical characterization of atmospheric particulate matter in China: A review. *Atmos. Environ.* **2017**, *158*, 270–304.
- (33) Heinritzi, M.; Simon, M.; Steiner, G.; Wagner, A. C.; Kürten, A.; Hansel, A.; Curtius, J. Characterization of the mass-dependent transmission efficiency of a CIMS. *Atmos. Meas. Tech.* **2016**, *9* (4), 1449–1460.
- (34) Fröhlich, R.; Cubison, M. J.; Slowik, J. G.; Bukowiecki, N.; Prévôt, A. S. H.; Baltensperger, U.; Schneider, J.; Kimmel, J. R.; Gonin, M.; Rohner, U.; Worsnop, D. R.; Jayne, J. T. The ToF-ACSM: a portable aerosol chemical speciation monitor with TOFMS detection. *Atmos. Meas. Tech.* **2013**, *6* (11), 3225–3241.
- (35) Canonaco, F.; Crippa, M.; Slowik, J. G.; Baltensperger, U.; Prévôt, A. S. H. SoFi, an IGOR-based interface for the efficient use of the generalized multilinear engine (ME-2) for the source apportion-

- ment: ME-2 application to aerosol mass spectrometer data. *Atmos. Meas. Tech.* **2013**, *6* (12), 3649–3661.
- (36) Boy, M.; Hellmuth, O.; Korhonen, H.; Nilsson, E. D.; ReVelle, D.; Turnipseed, A.; Arnold, F.; Kulmala, M. MALTE - model to predict new aerosol formation in the lower troposphere. *Atmos. Chem. Phys.* **2006**, *6* (12), 4499–4517.
- (37) Zha, Q.; Yan, C.; Junninen, H.; Riva, M.; Sarnela, N.; Aalto, J.; Quéléver, L.; Schallhart, S.; Dada, L.; Heikkinen, L.; Peräkylä, O.; Zou, J.; Rose, C.; Wang, Y.; Mammarella, I.; Katul, G.; Vesala, T.; Worsnop, D. R.; Kulmala, M.; Petäjä, T.; Bianchi, F.; Ehn, M. Vertical characterization of highly oxygenated molecules (HOMs) below and above a boreal forest canopy. *Atmos. Chem. Phys.* **2018**, *18* (23), 17437–17450.
- (38) Zaytsev, A.; Koss, A. R.; Breitenlechner, M.; Krechmer, J. E.; Nihill, K. J.; Lim, C. Y.; Rowe, J. C.; Cox, J. L.; Moss, J.; Roscioli, J. R.; Canagaratna, M. R.; Worsnop, D. R.; Kroll, J. H.; Keutsch, F. N. Mechanistic study of the formation of ring-retaining and ring-opening products from the oxidation of aromatic compounds under urban atmospheric conditions. *Atmos. Chem. Phys.* **2019**, *19* (23), 15117–15129.
- (39) Kroll, J. H.; Donahue, N. M.; Jimenez, J. L.; Kessler, S. H.; Canagaratna, M. R.; Wilson, K. R.; Altieri, K. E.; Mazzoleni, L. R.; Wozniak, A. S.; Bluhm, H.; Mysak, E. R.; Smith, J. D.; Kolb, C. E.; Worsnop, D. R. Carbon oxidation state as a metric for describing the chemistry of atmospheric organic aerosol. *Nat. Chem.* **2011**, *3*, 133.
- (40) McDonald, B. C.; de Gouw, J. A.; Gilman, J. B.; Jathar, S. H.; Akherati, A.; Cappa, C. D.; Jimenez, J. L.; Lee-Taylor, J.; Hayes, P. L.; McKeen, S. A.; Cui, Y. Y.; Kim, S.-W.; Gentner, D. R.; Isaacman-VanWertz, G.; Goldstein, A. H.; Harley, R. A.; Frost, G. J.; Roberts, J. M.; Ryerson, T. B.; Trainer, M. Volatile chemical products emerging as largest petrochemical source of urban organic emissions. *Science* **2018**, *359* (6377), 760–764.
- (41) Guenther, A.; Hewitt, C. N.; Erickson, D.; Fall, R.; Geron, C.; Graedel, T.; Harley, P.; Klinger, L.; Lerdau, M.; McKay, W. A.; Pierce, T.; Scholes, B.; Steinbrecher, R.; Tallamraju, R.; Taylor, J.; Zimmerman, P. A global model of natural volatile organic compound emissions. *J. Geophys. Res.* **1995**, *100* (D5), 8873–8892.
- (42) Schobesberger, S.; Junninen, H.; Bianchi, F.; Lonn, G.; Ehn, M.; Lehtipalo, K.; Dommen, J.; Ehrhart, S.; Ortega, I. K.; Franchin, A.; Nieminen, T.; Riccobono, F.; Hutterli, M.; Duplissy, J.; Almeida, J.; Amorim, A.; Breitenlechner, M.; Downard, A. J.; Dunne, E. M.; Flagan, R. C.; Kajos, M.; Keskinen, H.; Kirkby, J.; Kupc, A.; Kurten, A.; Kurten, T.; Laaksonen, A.; Mathot, S.; Onnela, A.; Praplan, A. P.; Rondo, L.; Santos, F. D.; Schallhart, S.; Schnitzhofer, R.; Sipila, M.; Tome, A.; Tsagkogeorgas, G.; Vehkamaki, H.; Wimmer, D.; Baltensperger, U.; Carslaw, K. S.; Curtius, J.; Hansel, A.; Petaja, T.; Kulmala, M.; Donahue, N. M.; Worsnop, D. R. Molecular understanding of atmospheric particle formation from sulfuric acid and large oxidized organic molecules. *Proc. Natl. Acad. Sci. U. S. A.* **2013**, *110* (43), 17223–8.
- (43) Ding, X.; Zhang, Y. Q.; He, Q. F.; Yu, Q. Q.; Wang, J. Q.; Shen, R. Q.; Song, W.; Wang, Y. S.; Wang, X. M. Significant Increase of Aromatics-Derived Secondary Organic Aerosol during Fall to Winter in China. *Environ. Sci. Technol.* **2017**, *51* (13), 7432–7441.
- (44) Li, M.; Zhang, Q.; Zheng, B.; Tong, D.; Lei, Y.; Liu, F.; Hong, C.; Kang, S.; Yan, L.; Zhang, Y.; Bo, Y.; Su, H.; Cheng, Y.; He, K. Persistent growth of anthropogenic non-methane volatile organic compound (NMVOC) emissions in China during 1990–2017: drivers, speciation and ozone formation potential. *Atmos. Chem. Phys.* **2019**, *19* (13), 8897–8913.
- (45) Donahue, N. M.; Kroll, J. H.; Pandis, S. N.; Robinson, A. L. A two-dimensional volatility basis set – Part 2: Diagnostics of organic-aerosol evolution. *Atmos. Chem. Phys.* **2012**, *12* (2), 615–634.
- (46) Donahue, N. M.; Epstein, S. A.; Pandis, S. N.; Robinson, A. L. A two-dimensional volatility basis set: 1. organic-aerosol mixing thermodynamics. *Atmos. Chem. Phys.* **2011**, *11* (7), 3303–3318.
- (47) Wang, J.; Ye, J.; Zhang, Q.; Zhao, J.; Wu, Y.; Li, J.; Liu, D.; Li, W.; Zhang, Y.; Wu, C.; Xie, C.; Qin, Y.; Lei, Y.; Huang, X.; Guo, J.; Liu, P.; Fu, P.; Li, Y.; Lee, H. C.; Choi, H.; Zhang, J.; Liao, H.; Chen, M.; Sun, Y.; Ge, X.; Martin, S. T.; Jacob, D. J. Aqueous production of secondary organic aerosol from fossil-fuel emissions in winter Beijing haze. *Proc. Natl. Acad. Sci. U. S. A.* **2021**, *118* (8), e2022179118.



JACS Au
AN OPEN ACCESS JOURNAL OF THE AMERICAN CHEMICAL SOCIETY

Editor-in-Chief
Prof. Christopher W. Jones
Georgia Institute of Technology, USA

Open for Submissions 

pubs.acs.org/jacsau ACS Publications
Most Trusted. Most Cited. Most Read.